MAX-PLANCK-INSTITUT FÜR PLASMAPHYSIK

GARCHING BEI MÜNCHEN

# A CALCULATION OF ELECTRON CYCLOTRON EMISSION LINE PROFILES FOR THE W VII - A STELLARATOR PLASMA

Z. X. ZHANG *

IPP 2/263 August 1982

Permanent Address : Institute of Physics, Academia Sinica. Now working in IPP as an Alexander von Humboldt Stipendiat.

*Die nachstehende Arbeit wurde im Rahmen des Vertrages zwischen dem Max-Planck-Institut für Plasmaphysik und der Europäischen Atomgemeinschaft über die Zusammenarbeit auf dem Gebiete der Plasmaphysik durchgeführt.*

Abstract

A three-dimensional ray-tracing code for the stellarator plasma is worked out. By an integration along its trace the ECE line profiles at the second harmonic for different W VII-A plasma parameters are calculated. Attention is paid especially to which line profile should be recorded by the diagnostics, the influence of the finite aperture of the antenna, the wave polarization and wall reflection are studied. The reliability of measuring temperature profiles by ECE line shape is discussed. The code can be used to calculate the expected ECE spectrum.

## 1. Introduction

Electron cyclotron emission measurements at W VII-A and at other machines using a Michelson interferometer have been carried through for a few years [1]. Electron cyclotron radiation at the second harmonic is recorded. Owing to the spatial variation of the magnetic field, the recorded intensity at the second harmonic has a profile with a frequency width which is much wider than the Doppler width. This line profile is interpreted as the electron temperature profile. To check the reliability of such estimation a previous work was done [2], which was a two-dimensional ray tracing, using Snell's law and cold plasma dispersion equation for the perpendicular propagation. The radiation from one poloidal plane only was considered. But the antenna (a circular horn) has some definite effective aperture. To study the effect of the antenna aperture is one of the purposes of the present work.

By Celata and Boyd [3] a code was described, which is based on an onedimensional slab model (only perpendicular propagation was considered) and calculates the ECE spectrum from a Tokamak plasma. The present work is mainly interested in the spectrum which should be recorded by the diagnostic equipment, therefore the calculation is carried out in a situation which is very close to experimental conditions. Since the present work is based on a three dimensional ray-tracing, it is possible to study the ECE radiation from any direction.

For every given frequency we first calculate 10 different ray traces (corresponding to antenna aperture), then we calculate the radiation from every trace and add them together according to appropriate weights (since the antenna has different magnification to the waves from different directions), in this way the intensity at this frequency is obtained. Then the procedure is repeated for another frequency. In this way a line profile (or a spectrum) is obtained. This profile is just the one which should be recorded by the interferometer.

## 2. Basic equations and procedure of calculation

The propagation and absorption of electron cyclotron radiation with frequency $\omega$ is governed by the following equation [4].

$$\frac{d}{ds}\left(\frac{I_\omega}{n_r^2}\right) = \frac{J_\omega}{n_r^2} - \alpha_\omega \left(\frac{I_\omega}{n_r^2}\right) \qquad (1)$$

where ds is the arc length along the ray trace , $n_r$ is the ray refractive index, $I_\omega$ is the intensity, $J_\omega$ is the emmissivity, $\alpha_\omega$ is the effective absorption coefficient.

Considering two points B and A on the ray, we can calculate the intensity at a point A from the known value at a preceding point B by the following formula, if these two points are close enough:

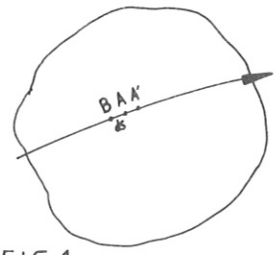

FIG.1

$$\frac{I_\omega(A)}{n_r^2(A)} = \frac{I_\omega(B)}{n_r^2(B)} e^{-\alpha_\omega ds} + \frac{T_e(A)\omega^2}{8\pi^3 C^2}\left(1 - e^{-\alpha_\omega ds}\right) \qquad (2)$$

As the next step A becomes the starting point, the intensity at a next point A' is calculated, and so on. The initial intensity at the starting point of the ray is zero, if wall reflections are not taken into account. The value of the ray refractive index outside the plasma is unity, so we need only to calculate $\alpha_\omega ds$ and $T_e$ in every step of doing the integration according to formula (2). Using such a procedure the intensity at $\omega$ from the considered ray is obtained.

For every given frequency ten rays are calculated. Their primary positions and primary propagating directions are shown in Fig. 2 (here the ray-tracing process is carried out by starting from the antenna as the initial point).

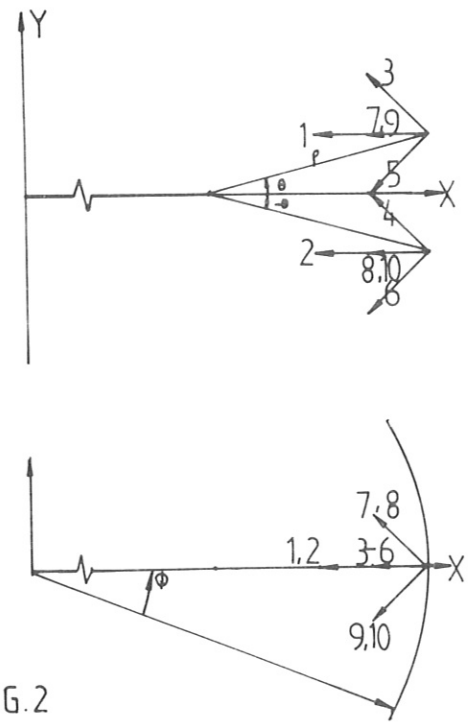


FIG.2

Rays 1 and 2 are in the x,y plane and are parallel to the equatorial plane. Rays 3,4,5,6 are in the x,y plane but with an obligue angle $\alpha$ to the equatorial plane. Rays 7,8,9,10 are oblique to the poloidal plane (x-y plane) by an angle $\alpha$ and are parallel to the equatorial plane.

As mentioned before, at a given frequency $\omega$ we obtain an intensity $I_\omega(L)$ for every ray L by an integration according to formula (2). Then we add the ten values of the $I_\omega(L)$ together according to their weights:

$$I_\omega = \sum_{L=1}^{10} I_\omega(L)\,G(L) \qquad (3)$$

where G(L) is the weight of the L-th ray and is given afterwards. $I_\omega$ is the spectral intensity at frequency $\omega$. To obtain the line profile at the second harmonic, 25 different frequencies are selected which correspond to the spatial variation of the magnetic field across the plasma cross-section. Then using an interpolation technique we obtain the calculated line profile as shown in the figures.

Weight $G(L) = R(L) / \sum_{L=1}^{10} R(L)$, R(L) are listed below for the case without polarization and wall reflection.

Table (1) weight values of the rays

| obligue angle $\alpha$ | $3^o$ | $5^o$ | $10^o$ | $15^o$ |
|---|---|---|---|---|
| R(1), R(2) | 1.0 | 1.0 | 1.0 | 1.0 |
| R(3), R(4), R(5) R(6) | .94 | .90 | .70 | .42 |
| R(7), R(8), R(9), R(10) | .94 | .90 | .70 | .42 |

In the code we calculate a relative temperature profile determined according to radiation intensity profile:

$$T_\omega = I_\omega / ( \omega^2 / 8\Pi^3 C^2 ) / T_o \quad ,$$

here $T_o$ is the temperature at the plasma centre.

When we integrate the radiation along its ray, we only do so within some limited range from $B(\omega) + \Delta B$ to $B(\omega)$ (for perpendicular propagating case) or from $B(\omega) + \Delta B$ to $B(\omega) - \Delta B$ (for obligue propagating case). Here $B(\omega)$ is the magnetic field at a point r on the considered ray where $2\omega_{ce}(r) = \omega$, $B(\omega) + \Delta B$ is the magnetic field at a point $r_1$ on the considered ray where $2\omega_{ce}(r_1) = \omega + 2\pi \times \Delta f$, similarly is $B(\omega) - \Delta B$. Here $\Delta f$ is the relativistic or Doppler line width [12]

$$\Delta f = 6.92 \times 10^{-6} \times f \times T_e \qquad (\text{for } N|\cos\beta| < V_t/c)$$

$$\Delta f = 3.51 \times 10^{-3} \times f \times T_e^{1/2} \times \cos\beta \quad (\text{for } N|\cos\beta| > V_t/c)$$

$$\Delta B = 1.786 \times 10^{-2} \times \Delta f$$

where f is in unit of GHz, $T_e$ is in eV, B is in Tesla, $\beta$ is the angle between the wave vector and the magnetic field, N is the refractive index, $V_t$ is the thermal velocity.

In the considered range of aperture (obligue angle < $15^o$) it is not necessary to include the contribution from o-mode at the second harmonic. The case with wall reflection is treated in section IV.

In the considered range of aperture, rays 1,2,3,4,5, and 6 correspond to the perpendicular propagation case ($N|\cos\beta| < V_t/c$); rays 7,8,9, and 10 correspond to oblique propagation case ($N|\cos\beta| > V_t/c$).

The coordinate system $(\rho,\theta,\varphi)$ for ray-tracing is shown in Fig. 3.

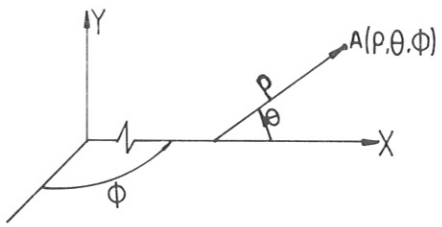


FIG.3

The equations used for ray tracing are [6,7]:

$$\frac{d\rho}{d\tau} = \frac{\partial g}{\partial k_\rho} \qquad \frac{dk_\rho}{d\tau} = -\frac{\partial g}{\partial \rho}$$

$$\frac{d\theta}{d\tau} = \frac{\partial g}{\partial m} \qquad \frac{dm}{d\tau} = -\frac{\partial g}{\partial \theta}$$

$$\frac{d\varphi}{d\tau} = \frac{\partial g}{\partial n} \qquad \frac{dn}{d\tau} = -\frac{\partial g}{\partial \varphi} \qquad (4)$$

where $k = (k_\rho, k_\theta, k_\varphi)$ is the wave vector, $m = \rho k_\theta$, $n = Rk_\varphi$, R is the major radius of the torus. $d\tau$ is a quantity which is proportional to the arc length along the ray, and

$$g \equiv 1 - W - XF^{-1} \quad (X,Y,s) \tag{5}$$

$$F = 1 - \frac{Y^2(1-S^2)}{2(1-X)} + M \cdot \frac{Y^2(1-S^2)}{2(1-X)} \times \left(1 + \frac{4S^2(1-X)}{Y^2(1-S^2)^2}\right)^{1/2} \tag{6}$$

$$X = \omega_p^2 / \omega^2 = 8.06 \times 10^3 \, n_e(\rho,\Theta,\varphi) / f^2 \tag{7}$$

$$Y = \omega_{ce} / \omega = 28.0 \times B(\rho,\Theta,\varphi) / f \tag{8}$$

$$S = \frac{c}{\omega} k_{\parallel} = 4.77 \times 10^{-2} \times (k_\rho B_\rho + m B_\Theta / \rho + B_\varphi n/R) \times B^{-1} \times f^{-1} \tag{9}$$

$$W = \frac{c^2}{\omega^2} k^2 = 2.28 \times 10^3 \times \left(k_\rho^2 + \left(\frac{m}{\rho}\right)^2 + \left(\frac{n}{R}\right)^2\right) \times f^{-2} \tag{10}$$

$M = +1$ for o-mode

$M = -1$ for x-mode

and f is in GHz, $n_e$ in $10^{20}/m^3$, B in Tesla. Function g comes from cold plasma dispersion equation - Appleton-Hartree equation [7]. For the fundamental mode and the n-th harmonic with $n > 2$, the warm plasma effect has only very little influence on the real part of the refractive index, so the cold plasma dispersion equation can be used for ray tracing in a warm plasma. But for the second harmonic at oblique propagation there is an upper density limit which is defined by

$$(\omega_p / 2\omega_{ce})^2 < 1 \tag{11}$$

Only below this limit the cold plasma model can be used for ray tracing for this mode in a warm plasma. As for the second harmonic of the x-mode at perpendicular propagation, a stronger upper density limit has to be set:

$$(\omega_p / \omega_{ce})^2 < 1 \tag{12}$$

The above ray-tracing procedure is a geometrical optics approximation, this approximation is valid if the plasma inhomogenity scale length and the damping length of the wave greatly exceed the wavelength. Above discussions are drawn from [8.9.13].

It is necessary to know the density distribution and the magnetic field vector at every point of the trace. For W VII-A we use following density distribution:

$$n_e(\rho,\theta,\varphi) \;/\; n_o \;=\; 1 \;/\; [1 + (X_H \;/P_H)^{Q_H}\;] \qquad (13)$$

where $P_H$, $Q_H$ are constants, $X_H$ is a function of $\rho$, $\theta$, and $\varphi$, its contours in poloidal plane are ellipses, rotating with toroidal angle $\varphi$ .

For the helical magnetic field we use a straight helical approximation [10]. The temperature distribution used for calculating absorption coefficient is

$$T_e(\rho,\theta,\varphi) \;/\; T_o \;=\; 1 \;/\; [\; 1 + \left(\frac{X_H}{X_T}\right)^{P_T}\;] \qquad (14)$$

where $X_T$ and $P_T$ are constants, $X_H$ is the same as in (13).

The formulas for calculating absorption coefficient $\alpha$ are taking from Ref. [11], or from Ref. [16] (Table 1, and formula 20, 21).

## 3. Calculated results

As mentioned in section (2), we call $T_\omega = I_\omega/(\omega^2/8\pi^3C^2)/T_o$ the relative temperature, where $I_\omega$ is the spectral intensity of electron cyclotron emission at frequency $\omega$. We draw the curve $T_\omega(X)$ versus X, here X is the horizontal coordinate of the plasma cross-section at $\varphi = 0$ plane where $2\omega_{ce}(X) = \omega$. We call this curve the relative temperature profile - RTP. We will mainly concentrate on a comparison between the RTP and the assumed temperature profile (formula 14).

A. At first let us see the influence of the effective aperture angle of the antenna radiation pattern. The RTP curves for different angles ($15^o$, $10^o$, $5^o$) are shown in Fig. 5, Fig. 7 and Fig. 9. The corresponding ray traces are shown in Fig. 4, Fig. 6 and Fig. 8. We can see that there is an abvious distortion in the RTP curve, compared with the assumed temperature profile when the antenna cone angle is $15^o$. When the antenna cone angle is $5^o$, the distortion is not large. If the effective angle of the used circular horn antenna is about $10^o$, the difference between the measured temperature profile and the real temperature profile is similar to the case shown in Fig. 7.

Further we would like to study where the distortion comes from. For this purpose the influence of the antenna aperture in different directions is studied. Fig. 10 and Fig. 11 show the results where the antenna has only an aperture along the poloidal plane and without any aperture along the equatorial plane. Fig. 12 and Fig. 13 show the results where the antenna has only an aperture along the equatorial plane and without any aperture along the poloidal plane. We can clearly see that the distortion of the RTP curve comes from the finite aperture in the poloidal plane. If the antenna aperture along the poloidal plane can be reduced, the coincidence between the measured temperature profile and the real temperature profile will be improved.

B. For every definite value of the magnetic field at the geometrical centre of the torus $B_o$, there exists an upper limit of the density value at plasma centre $n_{oc}$, when the plasma density at its centre $n_o$ is above this limit $n_{oc}$, the rays will be reflected by the plasma at some layer. In this case the RTP curve is seriously distorted and the measured result cannot be used to estimate electron temperature distribution at all. This situation is shown in Fig. 14 to Fig. 21.

The plasma reflection layer is determined by the cutoff condition:

$$\left(\frac{\omega_p}{\omega}\right)^2 = \left(1 - \left(\frac{k_{\parallel} C}{\omega}\right)^2\right) \cdot \left(1 - \frac{\omega_{ce}}{\omega}\right) \qquad (15)$$

A previous experiment showed that [14. Fig. 3] the ECE line shape changed when the plasma density increased. Now this phenomenon can be repeated by computer code.

We would like to point out that the wave cut-off condition in a cold plasma (formula 15, for x-mode) can only be used as a rough estimation to the working range of the ECE diagnostics. Because close to the cut-off density the rays are already considerably refracted, especially for the high magnetic field high density case.

C. When the density parameter $P_H$ (formula 13) is much less than the temperature parameter $X_T$ (formula 14), the RTP curve is much narrower than the assumed temperature profile, showed by Fig. 23 and Fig. 24, the corresponding ray trace. The reason is that the absorption coefficient is a function of $n_e \cdot T_e$. In the wing of the profile, plasma optical depth is not big enough, therefore recorded radiation intensity will decay following the decay of $T_e$ of $n_e$, depending on which one decays faster. Our calculations show that the width of the RTP curve is sensitive to the difference between parameters $P_H$ and $X_T$, but not sensitive to parameters $Q_H$ (formula 13) and $P_T$ (formula 14). If the temperature profile is already known

from another diagnostics, one can estimate density parameter $P_H$ according to the measured ECE line profile.

## 4. Effects of polarization and wall reflection

The polarization state of the radiated wave reaching the antenna is determined by the polarization state when the wave leaves the plasma boundary. For rays 1,2,3,4,5,6, which propagate almost perpendicular to magnetic field, we have [9] (about the meanings of the used symbols, please see the original paper):

$$E_z = 0 \qquad \frac{E_x}{E_y} = -\frac{i}{2}\left(\frac{\omega_p}{\omega_c}\right)^2 \frac{1 + 3N_\perp^2 F_{7/2}(Z_2)}{3 - \left(\frac{\omega_p}{\omega_c}\right)^2 \left[1 + \frac{3}{2} N_\perp^2 F_{7/2}(Z_2)\right]} \qquad (16)$$

At the plasma edge we have

$$E_x = E_z = 0 \qquad E_y \neq 0$$

Assuming the polarization axis of the receiver being perpendicular to the equatorial plane we have to modify the weight factors for rays 3,4,5, and 6 by a coefficient $\cos^2\alpha$ , here $\alpha$ is the obligue angle (the effective aperture angle of the antenna):

$$G(L) = R'(L) \Big/ \sum_{L=1}^{10} R'(L)$$

$$R'(L) = R(L) \cos^2\alpha \qquad L = 3,4,5,6$$

where R(L)'s are listed in Table 1.

For rays 7,8,9,10 which are propagating oblique to the magnetic field, we have [13] (n = 2 , about the meanings of the used symbols, please see the original paper).

$$E_x/E_y = i \cdot n \left[ 1 - \frac{n^2 - 1}{n^2} f_n(x) \right] \qquad (17)$$

$$E_x/E_z = - \frac{1 - (\omega_p/n\omega_c)^2 - N^2 \sin^2\beta}{N^2 \sin\beta \cos\beta} \qquad (18)$$

At plasma edge for different angle $\beta = 90^\circ - \alpha$ we have:

| $\alpha$ | $5^\circ$ | $10^\circ$ | $15^\circ$ |
|---|---|---|---|
| $E_x/E_y$ | $-1.46 \times 10^{-2} i$ | $-5.65 \times 10^{-2} i$ | $-1.15 \times 10^{-1} i$ |
| $E_x/E_z$ | $-8.70 \times 10^{-2}$ | $-1.76 \times 10^{-1}$ | $-2.68 \times 10^{-1}$ |
| $E_y/E_z$ | $-5.96 i$ | $-3.11 i$ | $-2.33 i$ |

We see that in the considered angle range $E_x << E_y$, $E_x << E_z$, wave is elliptically polarized in y-z plane. Again, assuming the polarization axis of the receiver being perpendicular to the equatorial plane, for the weight factors of the rays we have:

$$G(L) = R''(L) \Big/ \sum_L R''(L)$$

$$R''(L) = R(L) \cdot |E_y/E_z|^2 / (1 + |E_y/E_z|^2)$$

$$L = 7,8,9,10$$

where R(L)'s are listed in Table 1.

The calculated values of the ray weight are listed in Table 2:

| $\alpha$ | $5^{o}$ | $10^{o}$ | $15^{o}$ |
|---|---|---|---|
| R'(1) - R'(2) | 1.0 | 1.0 | 1.0 |
| R'(3) - R'(6) | .89 | .68 | .39 |
| R"(7) - R"(10) | .88 | .63 | .35 |

From a comparison of Table (1) and (2) we see that the polarization effect will not make any obvious influence to the line profile.

The wall reflection is treated by a manner which is similar to the treatment in [14]:

$$I_{\omega}(L) = \frac{T_e \omega^2}{8\pi^3 C^2} \frac{1 - e^{-\tau(\omega,L)}}{1 - \gamma e^{-\tau(\omega,L)}} \qquad (19)$$

where $T_e$ is the local temperature at the position on the ray where $B = 1.79 \times 10^{-2} \times \omega/2\pi$ ($\omega/2\pi$ in unit of GHz), $\gamma$ is the wall reflectivity. We calculate the optical length along the ray and obtain $\tau(\omega,L)$, then calculate $I_{\omega}(L)$ by using its corresponding value in the case without wall reflection, multiplied by a factor $1/(1 - \gamma \exp(-\tau(\omega,L)))$.

The calculated results are shown in Fig. 25, ($\gamma$ = 0.5), Fig. 26 ($\gamma$ = 0.8) and Fig. 27. After a comparison of Fig. 25 und Fig. 26 to Fig. 7 ($\gamma$ = 0) we cannot find obvious difference between these cases. This is because in this case most values of $\tau(\omega,L)$ are much bigger than 1. But when the density parameter $P_H$ is far from the temperature parameter $X_T$, the wall reflection will make an obvious change to the shape of the line profile. We can see this point from a comparison of Fig. 27 ($\gamma$ = 0.85) to Fig. 23 ($\gamma$ = 0).

## Conclusions

In order to make use of the measured ECE line profile at the second harmonic of extraordinary mode for measuring the electron temperature profile, the most important thing is to work in a parameter region without plasma cut-off layer to this mode. It is also very important to make the effective aperture of the antenna in the poloidal plane as small as possible (less than $5^{o}$). Up to a limit of $10^{o}$ the finite aperture of the antenna along the equatorial plane does not make any noticeable distortion to the line profile, when the axis of the horn is perpendicular to the magnetic field. When the ECE diagnostics is working at the second harmonic of extraordinary mode, the wall reflection will not make any obvious change to the shape of the line profile except that, the density profile is far from the temperature profile.

## Acknowledgement

This work is supported by Alexander von Humboldt-Stiftung and IPP. The author would like to express his acknowledge to Dr. G. von Gierke and Dr. H. Wobig for their much help. Special thanks to Dr. H. Wobig, Dr. M. Tutter and also to Dr. D. Campbell and Dr. F. Rau for many discussions. Dr. M. Tutter offered his original code to the author, which is a very valuable reference to the present work.

Figure Captions

The meanings of used symbols in all the figures are listed below.

BO : magnetic field at the geometrical centre of the machine, in Tesla

NO: electron density at plasma centre, in $10^{20}/m^3$

TO: electron temperature at plasma centre, in eV

HI: electric current in every bundle of the helical winding

DEN. PROF.: The three numbers written in this line are density parameters, the first is $P_H$, the second is $Q_H$ (see formula 13), the third one without any meaning in the present calculation.

TEM. PROF.: The three numbers listed in this line are temperature parameters, the first is $X_T$, the second is $P_T$ (see formula 14), the third one without any meaning in the present calculation.

HSH: plasma horizontal displacement

YSH: vertical displacement of the plasma centre

Fig. 4, 6, 8, 10, 12, 14, 16, 18, 20, 24:

These figures are ray tracing figures for the noticed wave frequency. The real line circle on the right picture is the plasma boundary. The three elliptical real lines are density contours which are corresponding to 0.75 $n_o$, 0.50 $n_o$ and 0.25 $n_o$, respectively. The cross mark on a ray designates the position where $2\omega_{ce} = \omega$. If there is not a cross mark on a ray, that means this ray has not reached the resonance layer of this noticed frequency $\omega$ before it goes out of the plasma region.

RADIUS IN CM: This is $\rho \cos \theta$. The another coordinate axis of the right picture of every tracing figure is $\rho \sin \theta$ .

ANGFAI IN DEGREE: this is the $\varphi$-coordinate of the trace in unite of degree (the definition of $\varphi$ is shown in Fig. 3).

Fig. 5, 7, 9, 11, 13, 15, 17, 19, 21, 23, 25, 26, 27:

These figures are curves of relative temperature versus coordinate $X = \rho \cos \theta$ at $\varphi = 0$ plane. The dotted line on every figure is the assumed temperature profile.

References

[1] Costley, A. E., Hastie, R. J., Paul. J. W. M., Chamberlain, J., Phys. Rev. Lett. 33 (1974), 758
TFR Group, NPL Submillimeter-Wave Group, in controlled Fusion and Plasma Physics (Proc. 7th Europ. Conf. Lausanne (1975), paper 14a
TFR Group, ibid. paper 14b
Cavallo, A., Tutter M., IPP 2/244 (1978)
W-VIIA Team (presented by D. V. Bartlett). The 5th Int. Conf. on Infrared and Mill. Waves, 1980.

[2] Tutter, M., a paper presented at DPG conference Würzburg (March) 1982

[3] Celata, C. M., Boyd, D. A., Nuclear Fusion 17 (1977), 735

[4] Bekefi, G., Radiation Processes in Plasmas, p. 38

[5] Jasik, H., Antenna Engineering Handbook, p. 10 - 12

[6] Stix, T. H., The Theory of Plasma Waves, p. 58

[7] Ott, E., Hui, B., Chu, K. R., Phys. Fluids 23 (1980), 1031

[8] Fidone, I., Granate, G., Ramponi, G., Phys. Fluids, 21 (1978), 645

[9] Bornatici, M., Dielectric Effects in the Electron Cyclotron Absorption, I. R. 80/023

[10] Morozov, A. I., Solovev, L. S., The Structure of Magnetic Fields, p. 42

[11] Bornatici, M., Engelmann, F., Novack, S., Petrillo, V., I. R. 81/016

[12] Engelmann, F., Curatolo, M., Nuclear Fusion, 13 (1973), 497

[13] Bornatici, M., Proceedings of the Joint Workshop on Electron Cyclotron Emission and Electron Cyclotron Resonance Heating, Oxford, Culham Report CLM-ECR (1980)

[14] Hutchinson, J. H., Komm, D. S., Nuclear Fusion 17 (1977), 1077

[15] Jäckel, H. J., Kißlinger, J., Rau, F., IPP 2/231, 1976

[16] Bornatici, M., Plasma Physics, 24 (1982), 629

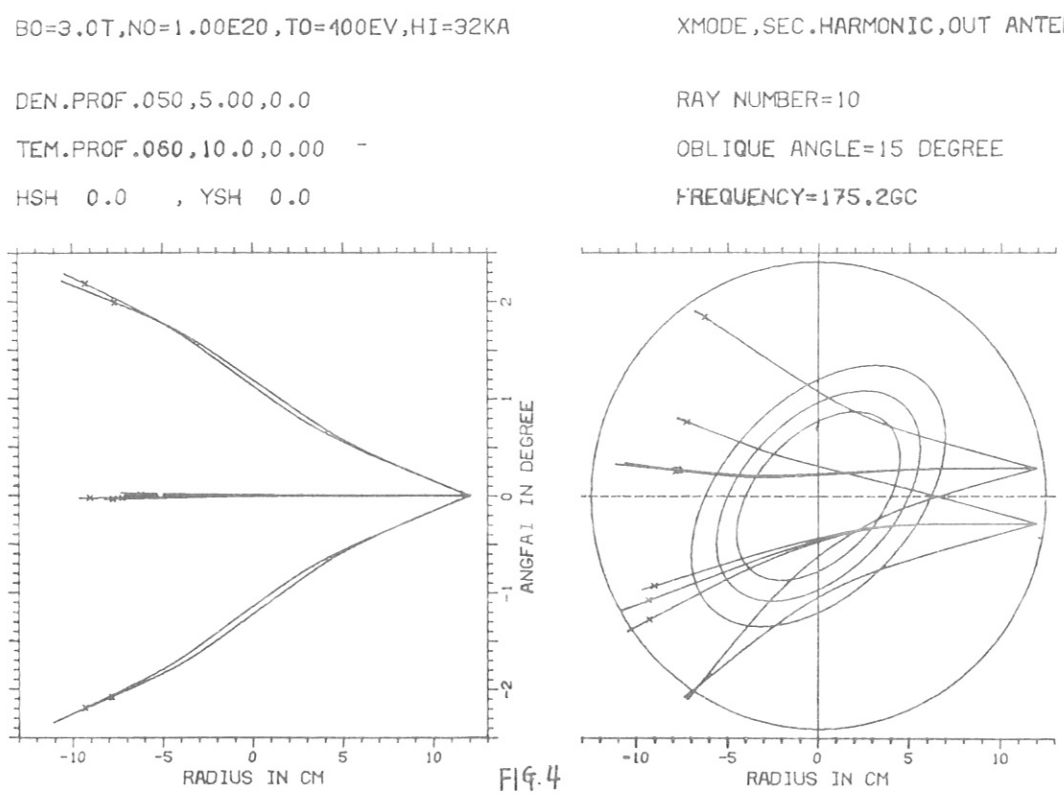
BO=3.0T,NO=1.00E20,TO=400EV,HI=32KA
DEN.PROF.050,5.00,0.0
TEM.PROF.060,10.0,0.00
HSH 0.0 , YSH 0.0
XMODE,SEC.HARMONIC,OUT ANTENA
RAY NUMBER=10
OBLIQUE ANGLE=15 DEGREE
FREQUENCY=175.2GC
ANGFAI IN DEGREE
RADIUS IN CM
RADIUS IN CM

FIG.4

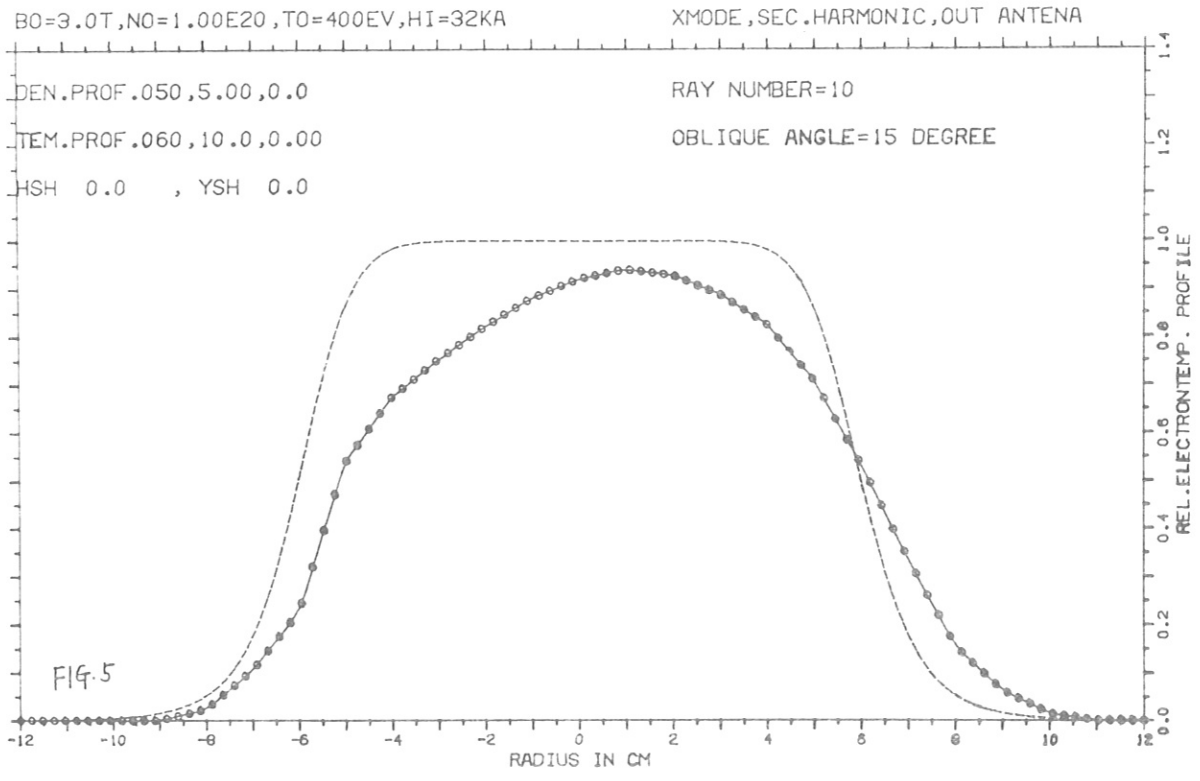
BO=3.0T,NO=1.00E20,TO=400EV,HI=32KA
DEN.PROF.050,5.00,0.0
TEM.PROF.060,10.0,0.00
HSH 0.0 , YSH 0.0
XMODE,SEC.HARMONIC,OUT ANTENA
RAY NUMBER=10
OBLIQUE ANGLE=15 DEGREE
REL.ELECTRONTEMP. PROFILE
RADIUS IN CM

FIG.5

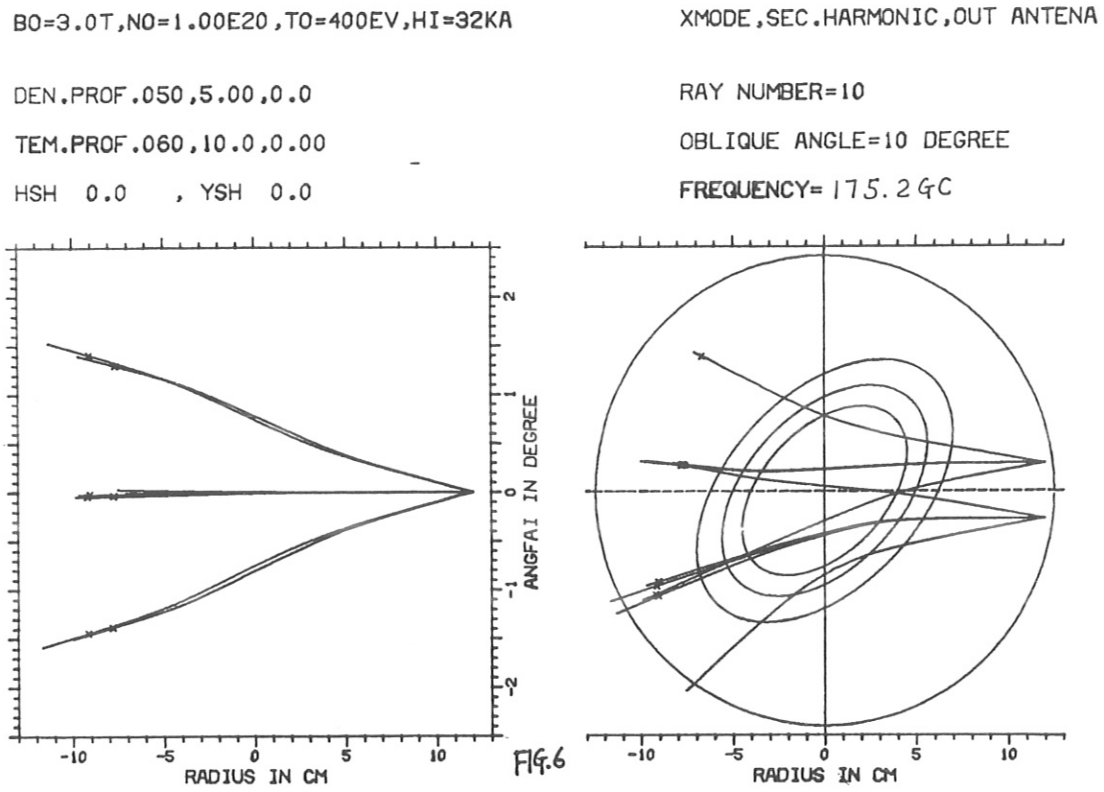
BO=3.0T,NO=1.00E20,TO=400EV,HI=32KA
DEN.PROF.050,5.00,0.0
TEM.PROF.060,10.0,0.00
HSH 0.0 , YSH 0.0
XMODE,SEC.HARMONIC,OUT ANTENA
RAY NUMBER=10
OBLIQUE ANGLE=10 DEGREE
FREQUENCY= 175.2GC
ANGFAI IN DEGREE
RADIUS IN CM
RADIUS IN CM

FIG.6

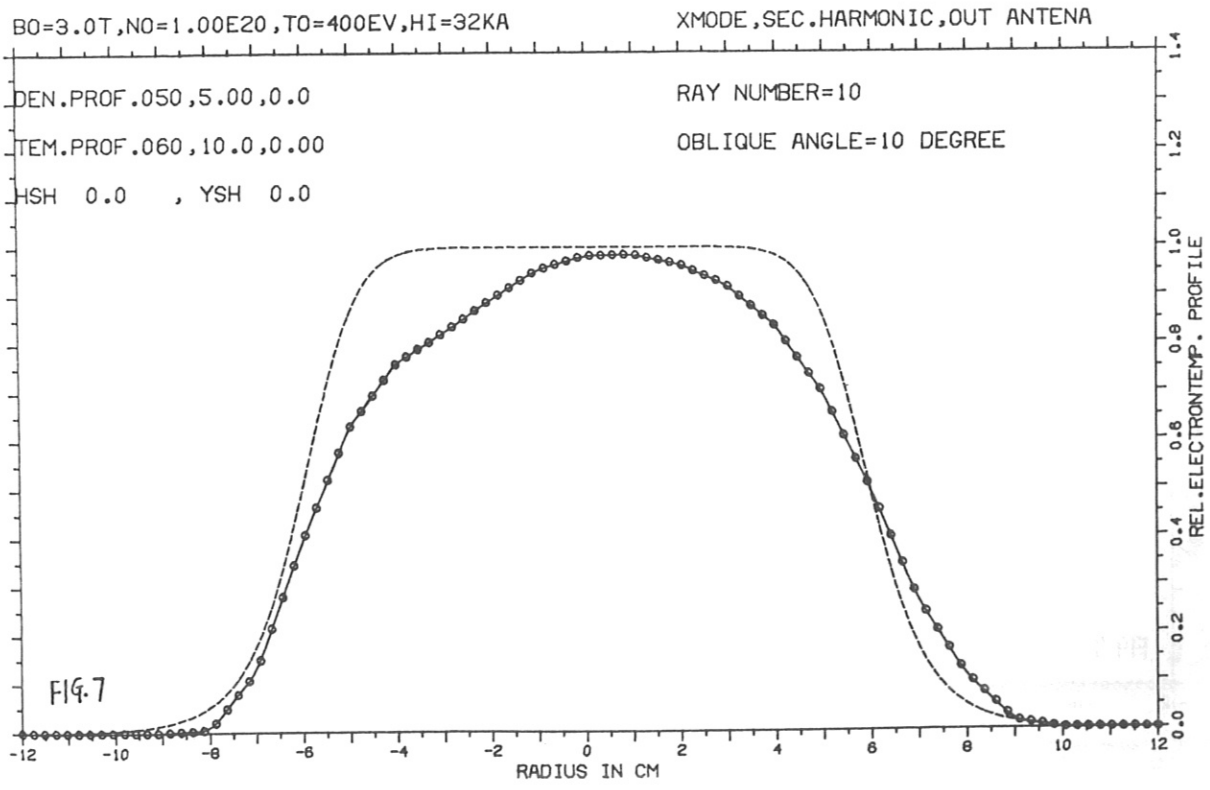
BO=3.0T,NO=1.00E20,TO=400EV,HI=32KA
DEN.PROF.050,5.00,0.0
TEM.PROF.060,10.0,0.00
HSH 0.0 , YSH 0.0
XMODE,SEC.HARMONIC,OUT ANTENA
RAY NUMBER=10
OBLIQUE ANGLE=10 DEGREE
REL.ELECTRONTEMP. PROFILE
RADIUS IN CM

FIG.7

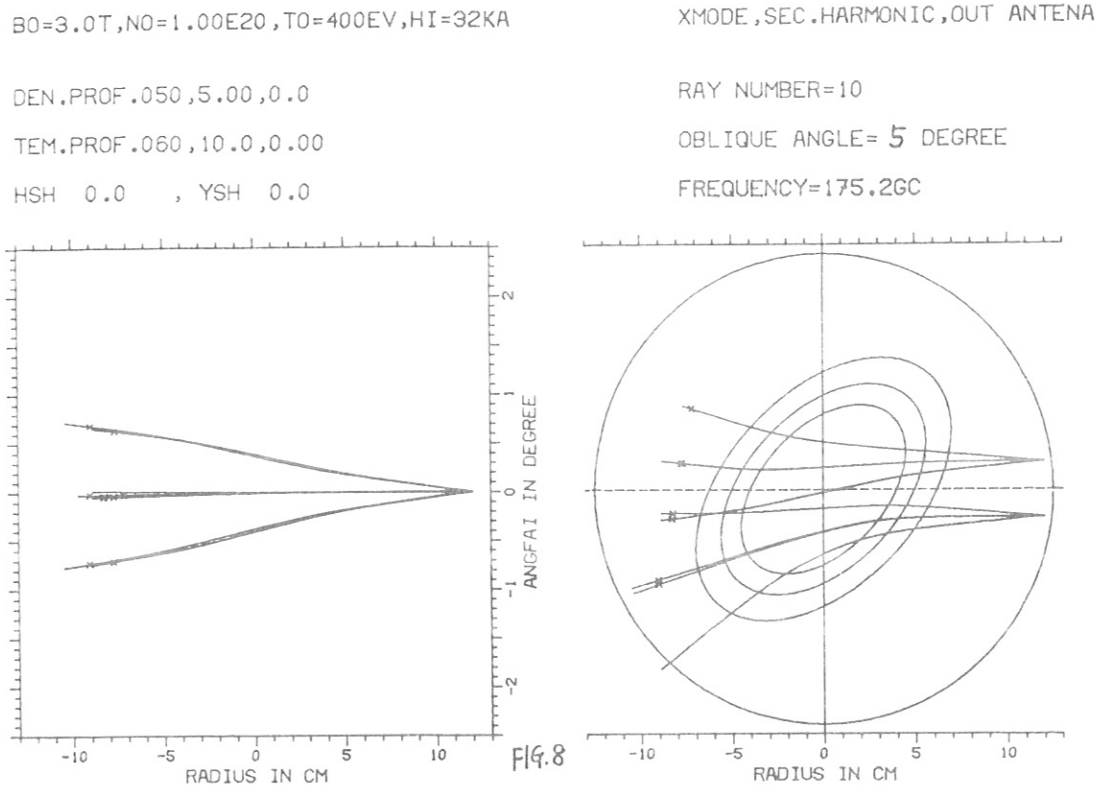
B0=3.0T,N0=1.00E20,T0=400EV,HI=32KA
DEN.PROF.050,5.00,0.0
TEM.PROF.060,10.0,0.00
HSH 0.0 , YSH 0.0
XMODE,SEC.HARMONIC,OUT ANTENA
RAY NUMBER=10
OBLIQUE ANGLE= 5 DEGREE
FREQUENCY=175.2GC
ANGFAI IN DEGREE
RADIUS IN CM
RADIUS IN CM

FIG.8

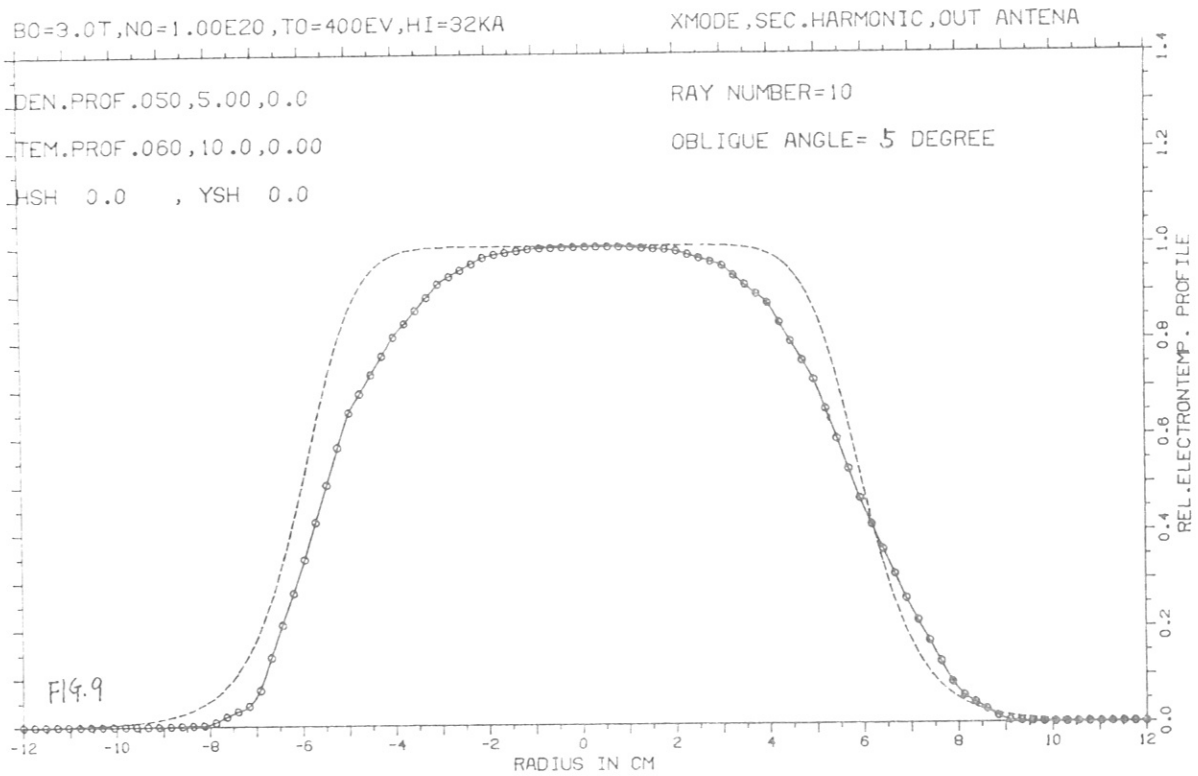
B0=3.0T,N0=1.00E20,T0=400EV,HI=32KA
DEN.PROF.050,5.00,0.0
TEM.PROF.060,10.0,0.00
HSH 0.0 , YSH 0.0
XMODE,SEC.HARMONIC,OUT ANTENA
RAY NUMBER=10
OBLIQUE ANGLE= 5 DEGREE
REL.ELECTRONTEMP. PROFILE
RADIUS IN CM

FIG.9

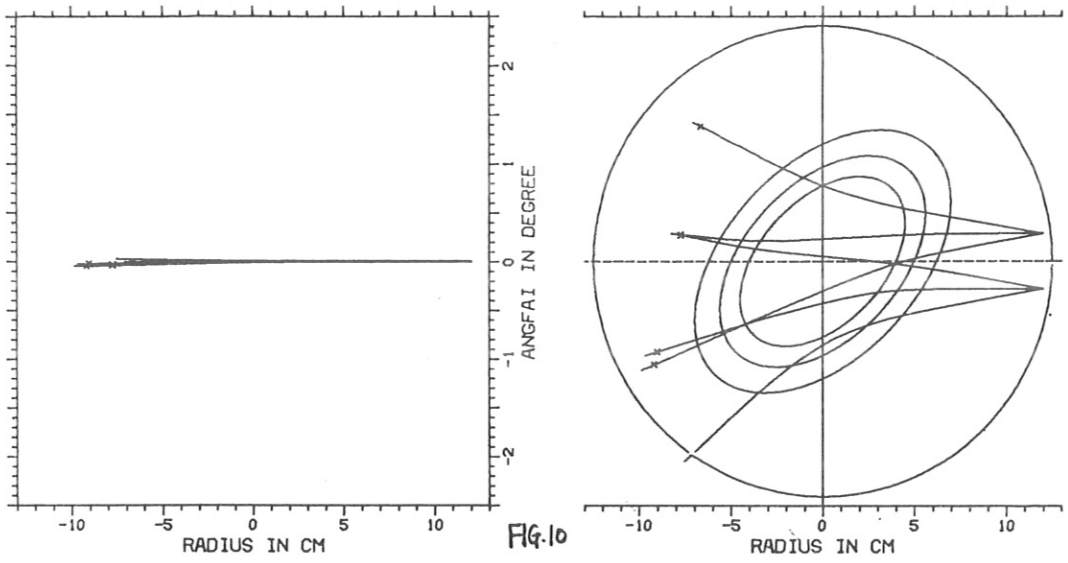
BO=3.0T,NO=1.00E20,TO=400EV,HI=32KA
DEN.PROF.050,5.00,0.0
TEM.PROF.060,10.0,0.00
HSH 0.0 , YSH 0.0
XMODE,SEC.HARMONIC,OUT ANTENA
RAY NUMBER= 6
OBLIQUE ANGLE=10 DEGREE
FREQUENCY=175.2GC
ANGFAI IN DEGREE
RADIUS IN CM
RADIUS IN CM

FIG.10

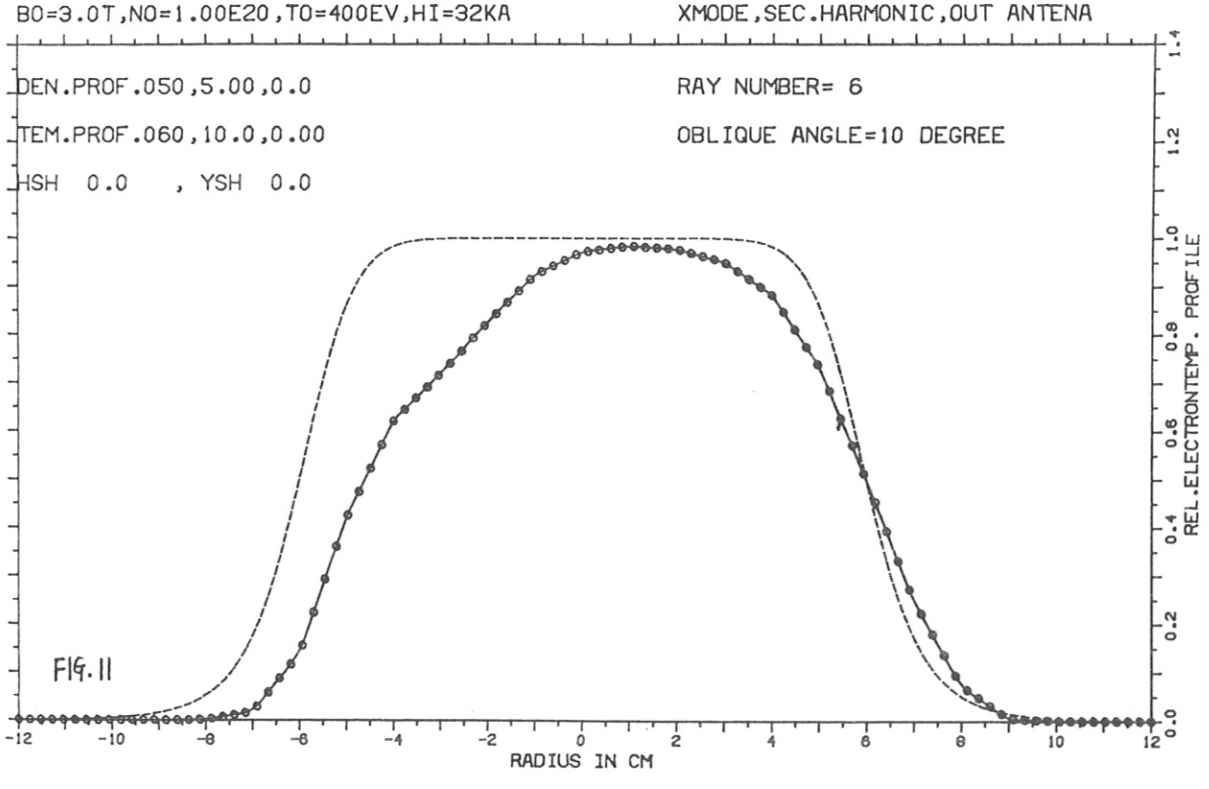
BO=3.0T,NO=1.00E20,TO=400EV,HI=32KA
DEN.PROF.050,5.00,0.0
TEM.PROF.060,10.0,0.00
HSH 0.0 , YSH 0.0
XMODE,SEC.HARMONIC,OUT ANTENA
RAY NUMBER= 6
OBLIQUE ANGLE=10 DEGREE
REL.ELECTRONTEMP. PROFILE
RADIUS IN CM

FIG.11

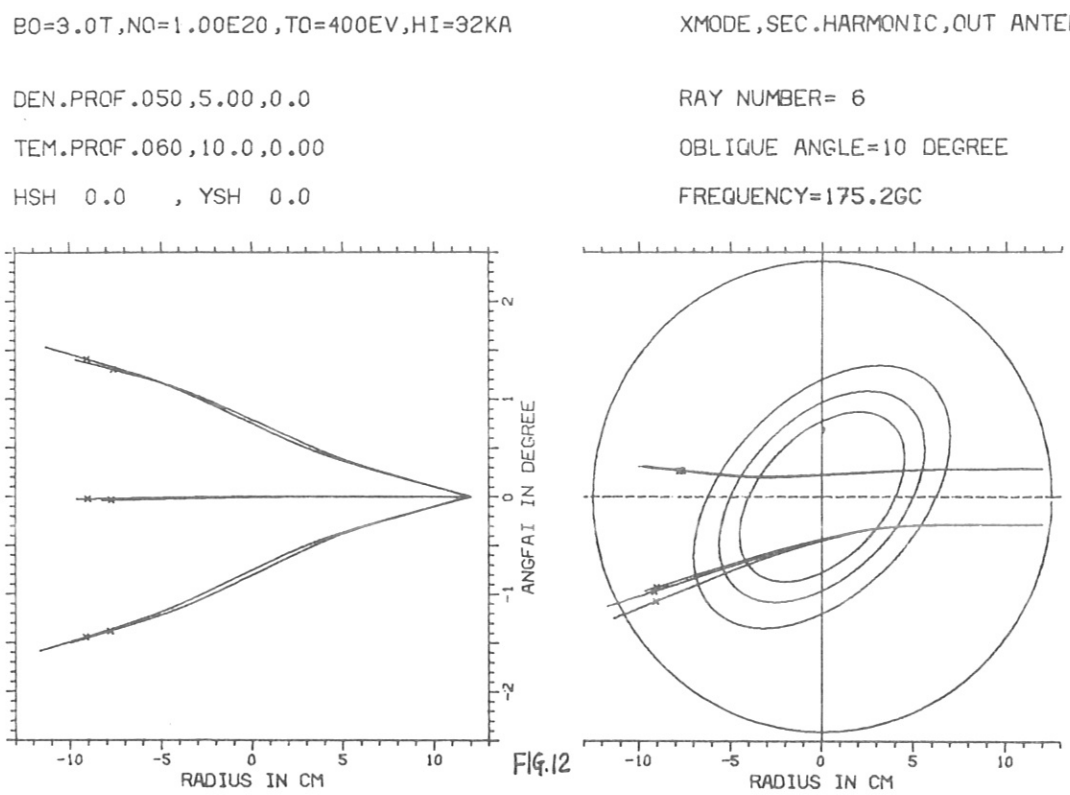
BO=3.0T,NO=1.00E20,TO=400EV,HI=32KA
DEN.PROF.050,5.00,0.0
TEM.PROF.060,10.0,0.00
HSH 0.0 , YSH 0.0
XMODE,SEC.HARMONIC,OUT ANTENA
RAY NUMBER= 6
OBLIQUE ANGLE=10 DEGREE
FREQUENCY=175.2GC
ANGFAI IN DEGREE
RADIUS IN CM
RADIUS IN CM

FIG.12

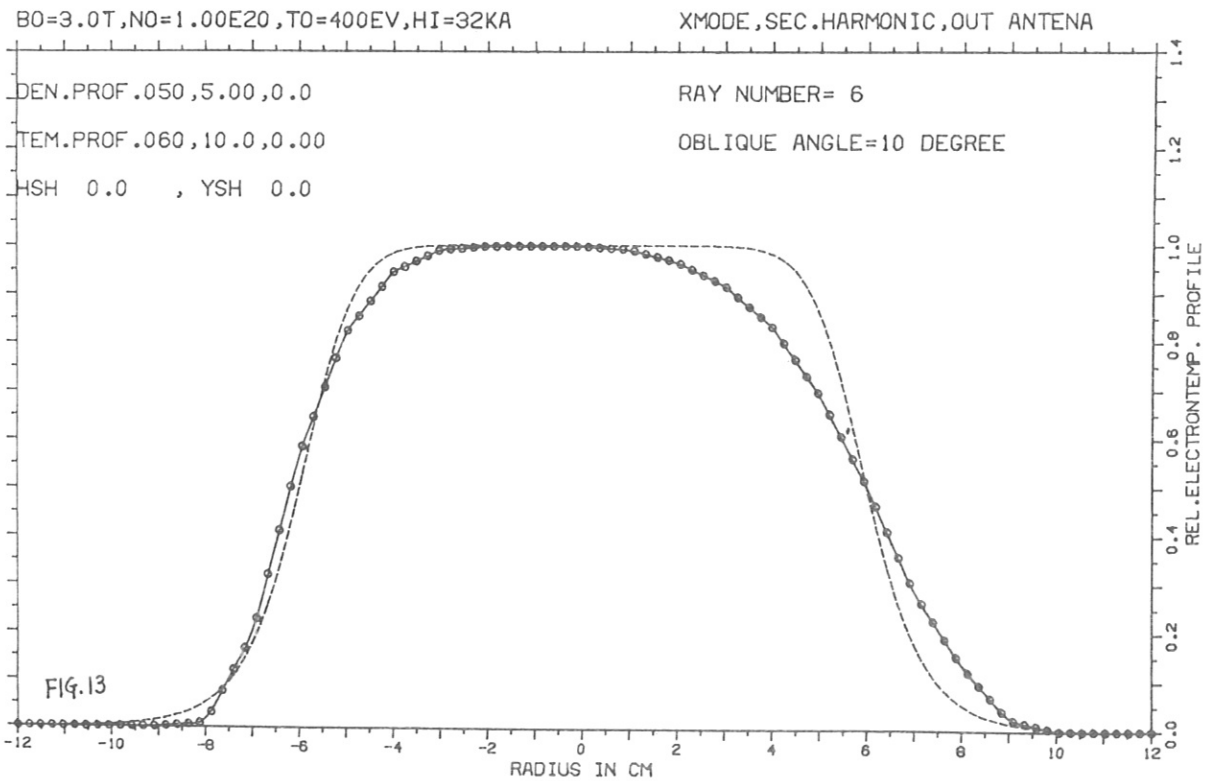
BO=3.0T,NO=1.00E20,TO=400EV,HI=32KA
DEN.PROF.050,5.00,0.0
TEM.PROF.060,10.0,0.00
HSH 0.0 , YSH 0.0
XMODE,SEC.HARMONIC,OUT ANTENA
RAY NUMBER= 6
OBLIQUE ANGLE=10 DEGREE
REL.ELECTRONTEMP. PROFILE
RADIUS IN CM

FIG.13

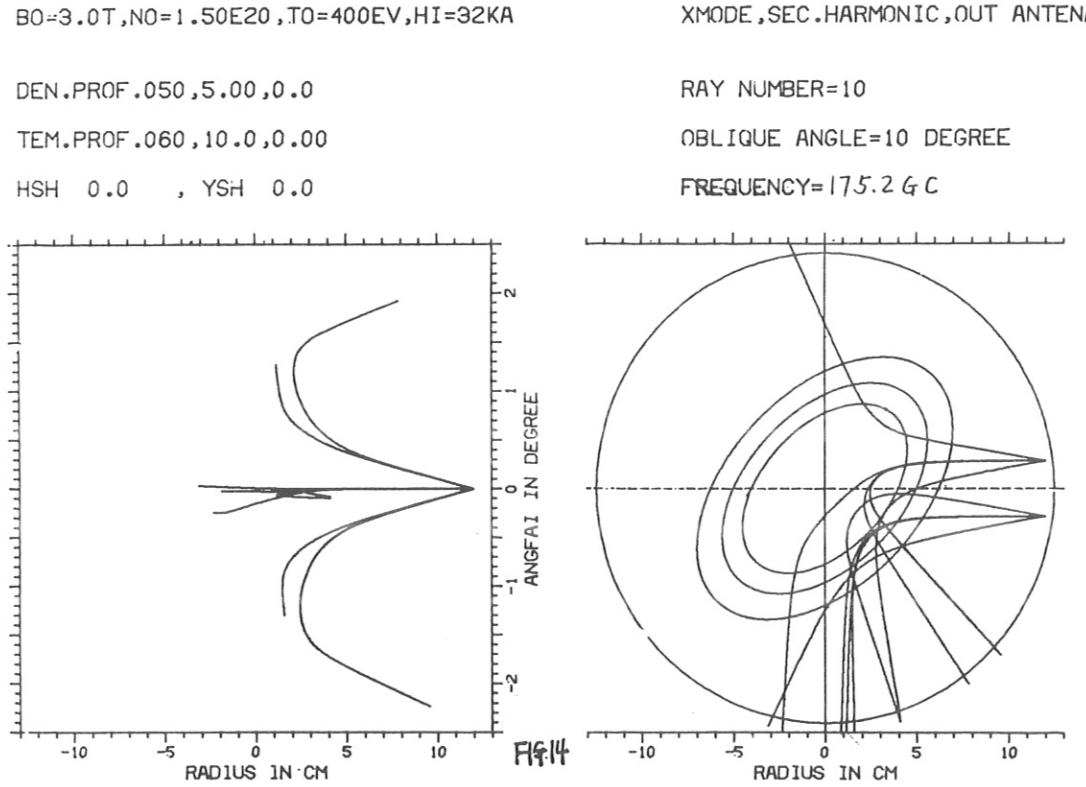
BO=3.0T,NO=1.50E20,TO=400EV,HI=32KA
DEN.PROF.050,5.00,0.0
TEM.PROF.060,10.0,0.00
HSH 0.0 , YSH 0.0
XMODE,SEC.HARMONIC,OUT ANTENA
RAY NUMBER=10
OBLIQUE ANGLE=10 DEGREE
FREQUENCY=175.2 GC
ANGFAI IN DEGREE
RADIUS IN CM
RADIUS IN CM

FIG.14

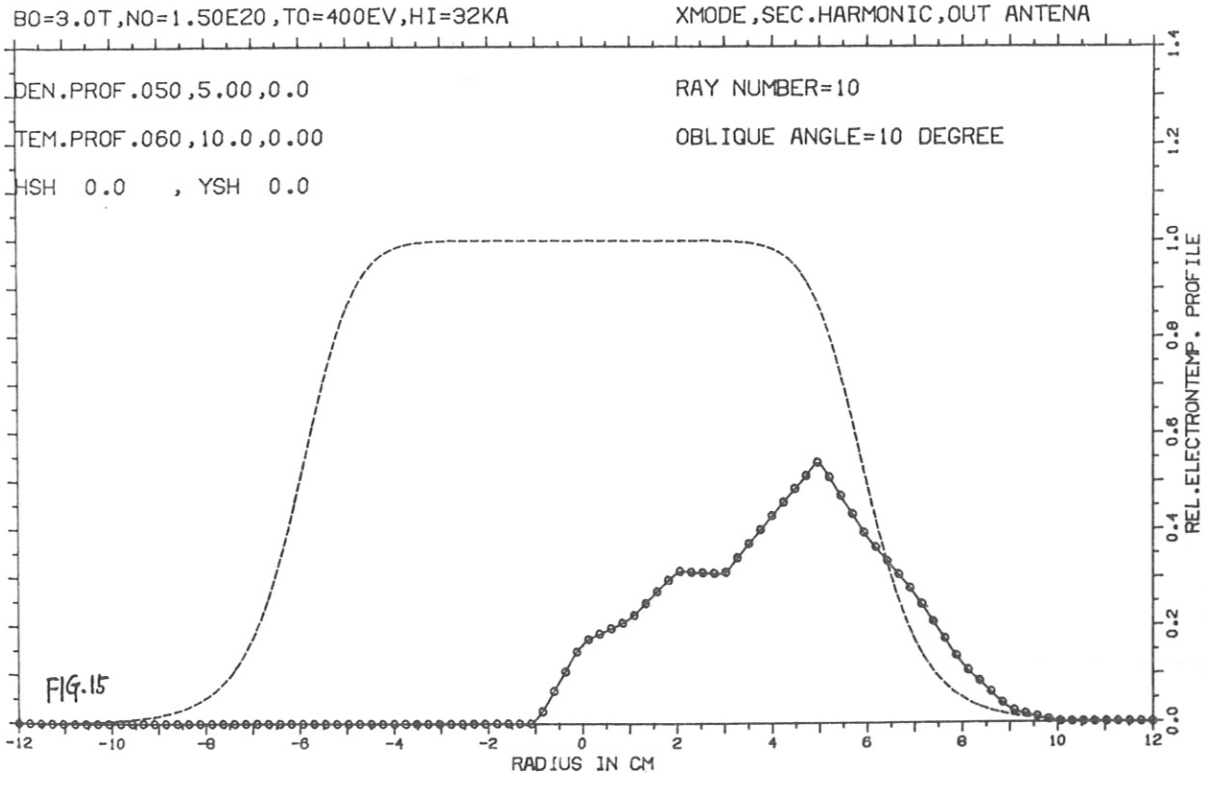
BO=3.0T,NO=1.50E20,TO=400EV,HI=32KA
DEN.PROF.050,5.00,0.0
TEM.PROF.060,10.0,0.00
HSH 0.0 , YSH 0.0
XMODE,SEC.HARMONIC,OUT ANTENA
RAY NUMBER=10
OBLIQUE ANGLE=10 DEGREE
REL.ELECTRONTEMP. PROFILE
RADIUS IN CM

FIG.15

BO=3.0T,NO=1.30E20,TO=400EV,HI=32KA

DEN.PROF.050,5.00,0.0

TEM.PROF.060,10.0,0.00

HSH 0.0 , YSH 0.0

XMODE,SEC.HARMONIC,OUT ANTENA

RAY NUMBER=10

OBLIQUE ANGLE=10 DEGREE

FREQUENCY=175.2GC

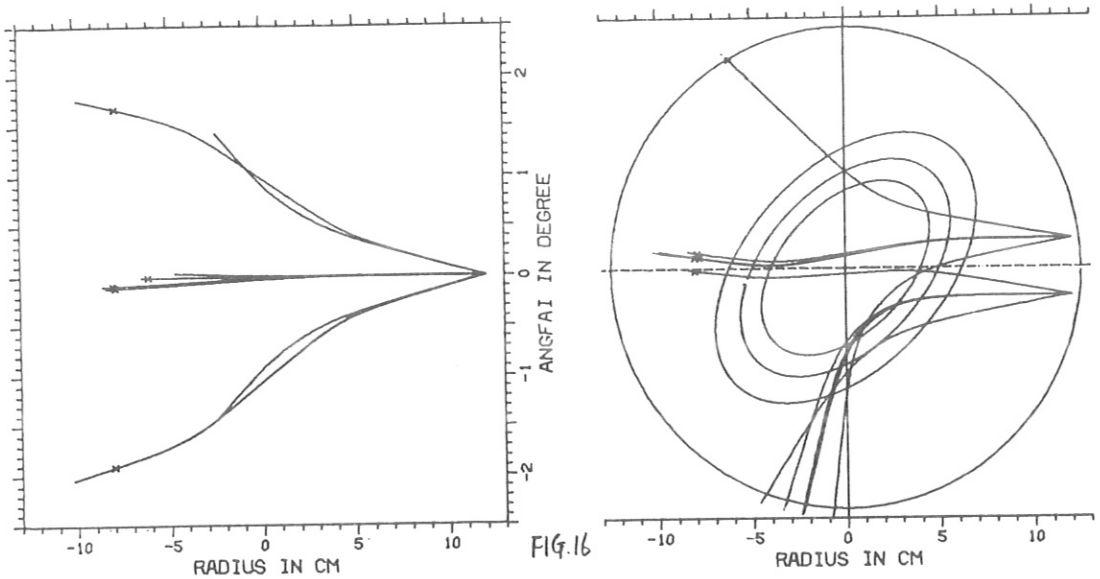


FIG.16

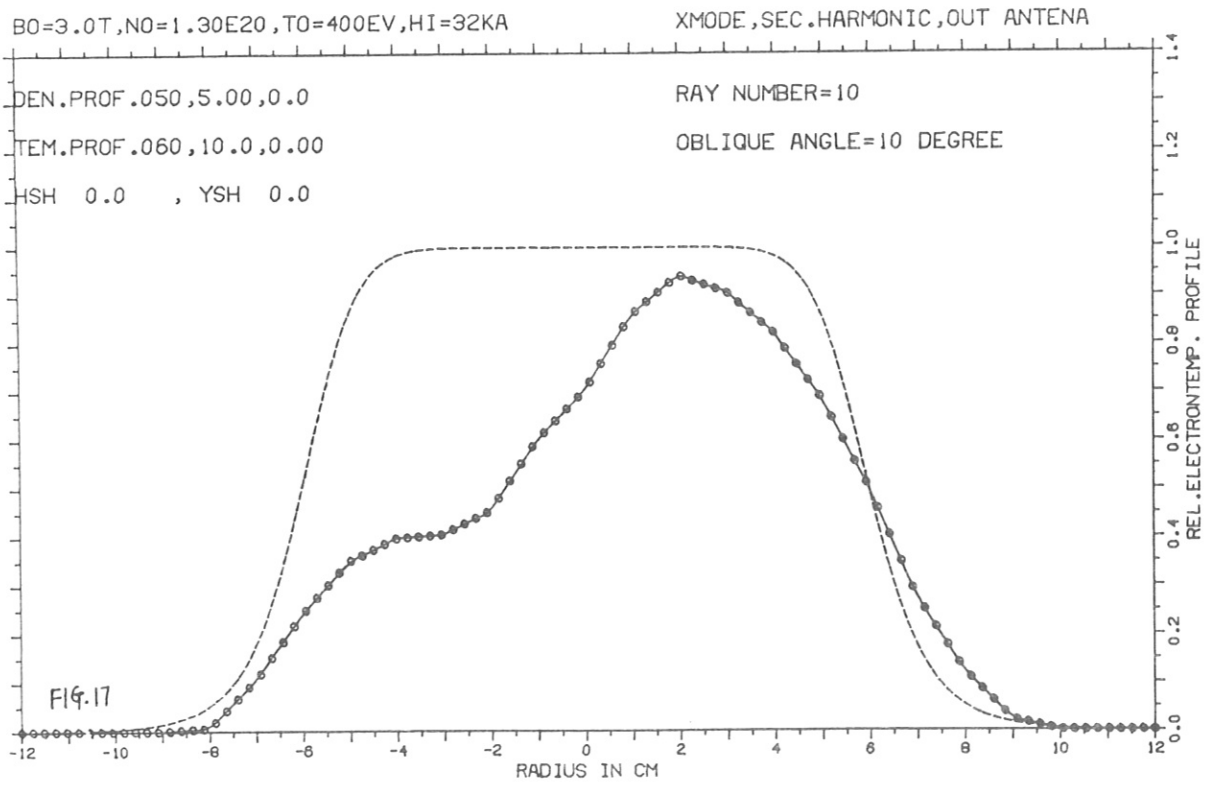


FIG.17

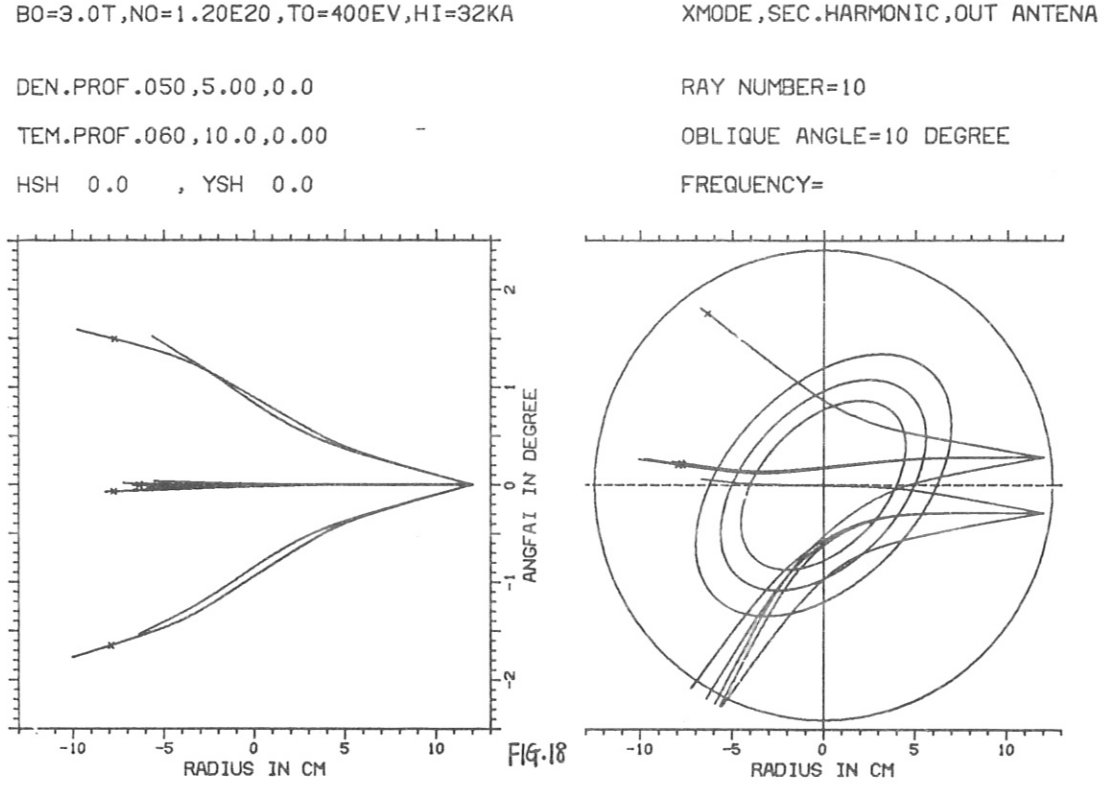
BO=3.0T,NO=1.20E20,TO=400EV,HI=32KA
DEN.PROF.050,5.00,0.0
TEM.PROF.060,10.0,0.00
HSH 0.0 , YSH 0.0
XMODE,SEC.HARMONIC,OUT ANTENA
RAY NUMBER=10
OBLIQUE ANGLE=10 DEGREE
FREQUENCY=
ANGFAI IN DEGREE
RADIUS IN CM
RADIUS IN CM

FIG.18

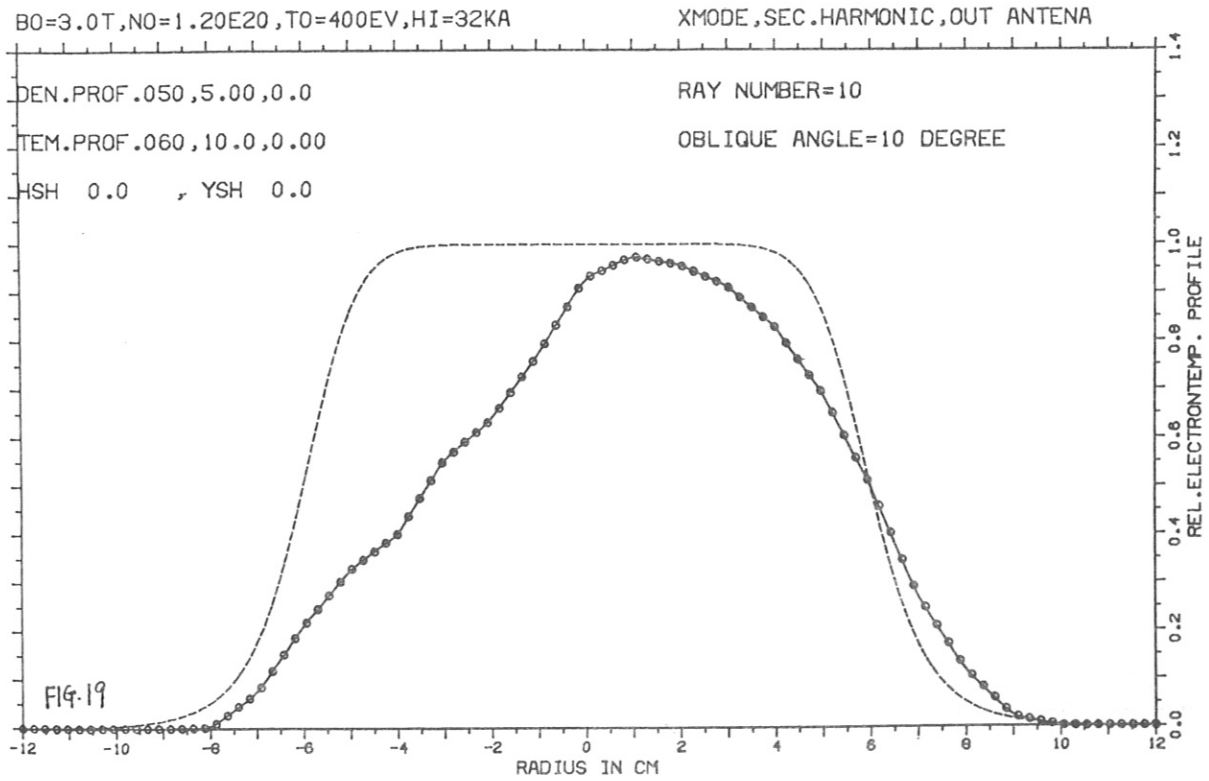
BO=3.0T,NO=1.20E20,TO=400EV,HI=32KA
DEN.PROF.050,5.00,0.0
TEM.PROF.060,10.0,0.00
HSH 0.0 , YSH 0.0
XMODE,SEC.HARMONIC,OUT ANTENA
RAY NUMBER=10
OBLIQUE ANGLE=10 DEGREE
REL.ELECTRONTEMP. PROFILE
RADIUS IN CM

FIG.19

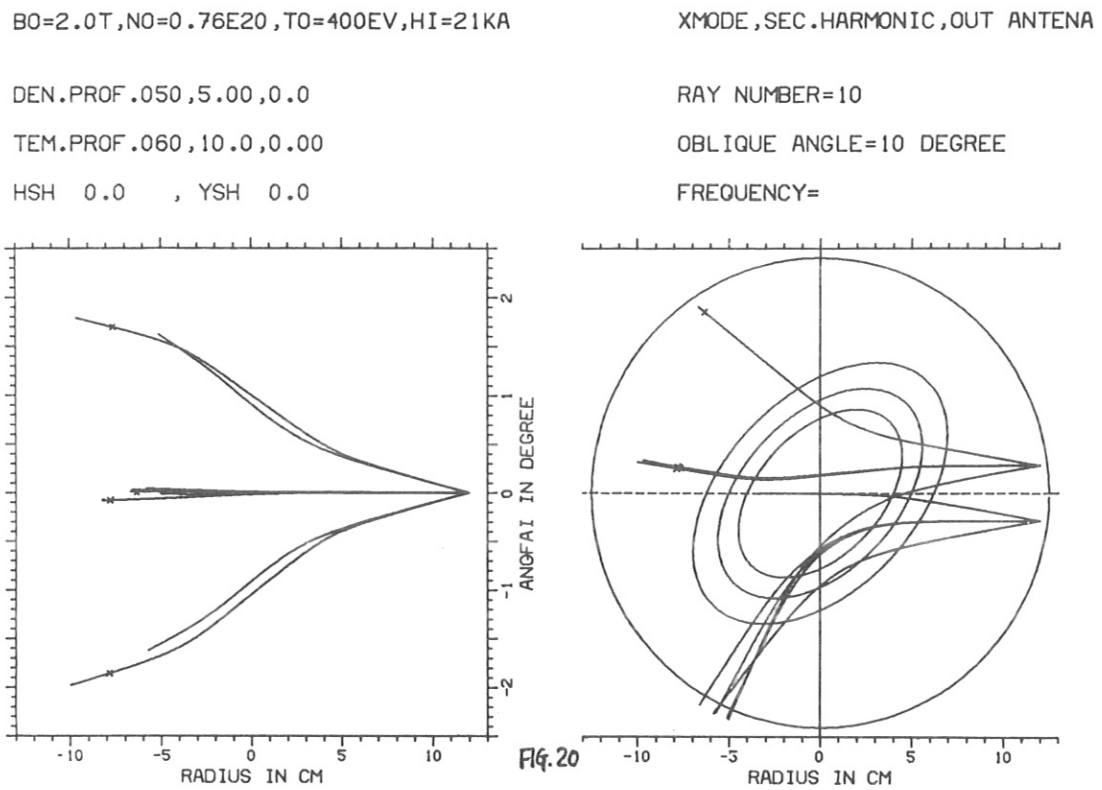
BO=2.0T,NO=0.76E20,TO=400EV,HI=21KA
DEN.PROF.050,5.00,0.0
TEM.PROF.060,10.0,0.00
HSH 0.0 , YSH 0.0
XMODE,SEC.HARMONIC,OUT ANTENA
RAY NUMBER=10
OBLIQUE ANGLE=10 DEGREE
FREQUENCY=
ANGFAI IN DEGREE
RADIUS IN CM
RADIUS IN CM

FIG. 20

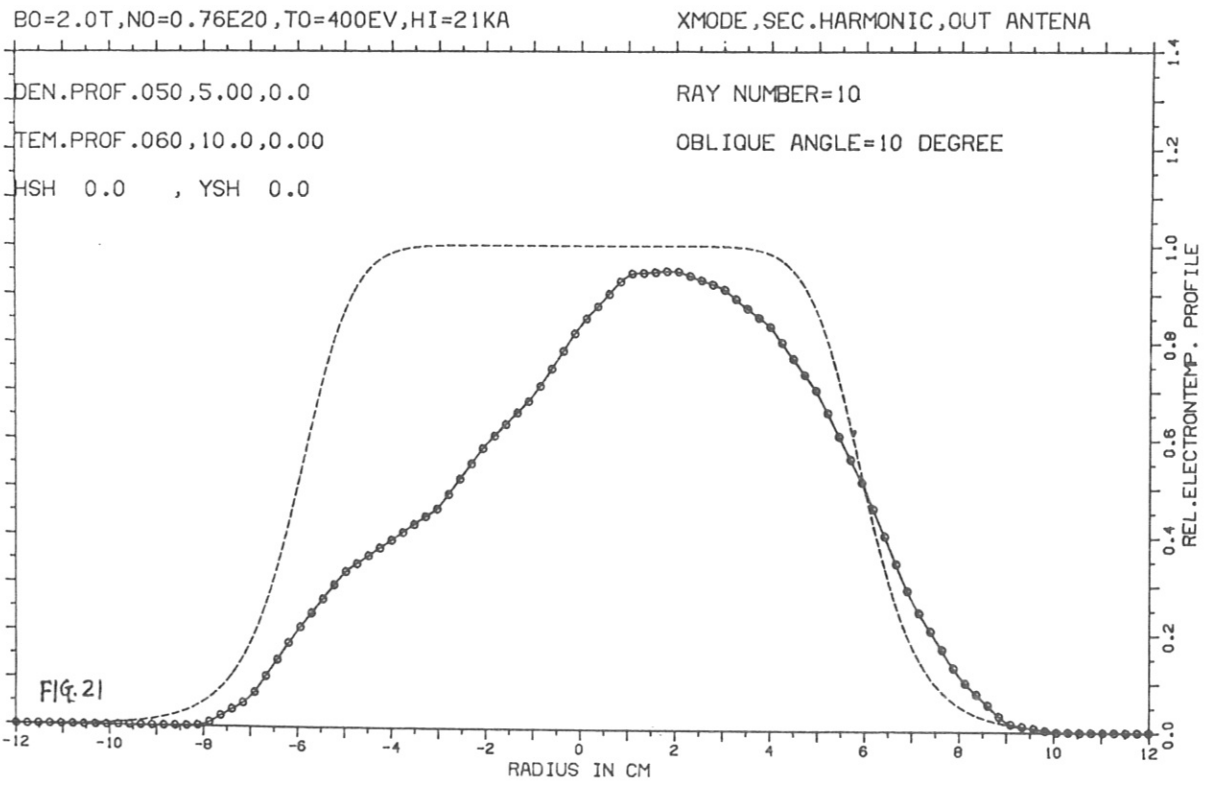
BO=2.0T,NO=0.76E20,TO=400EV,HI=21KA
DEN.PROF.050,5.00,0.0
TEM.PROF.060,10.0,0.00
HSH 0.0 , YSH 0.0
XMODE,SEC.HARMONIC,OUT ANTENA
RAY NUMBER=10
OBLIQUE ANGLE=10 DEGREE
REL.ELECTRONTEMP. PROFILE
RADIUS IN CM

FIG. 21

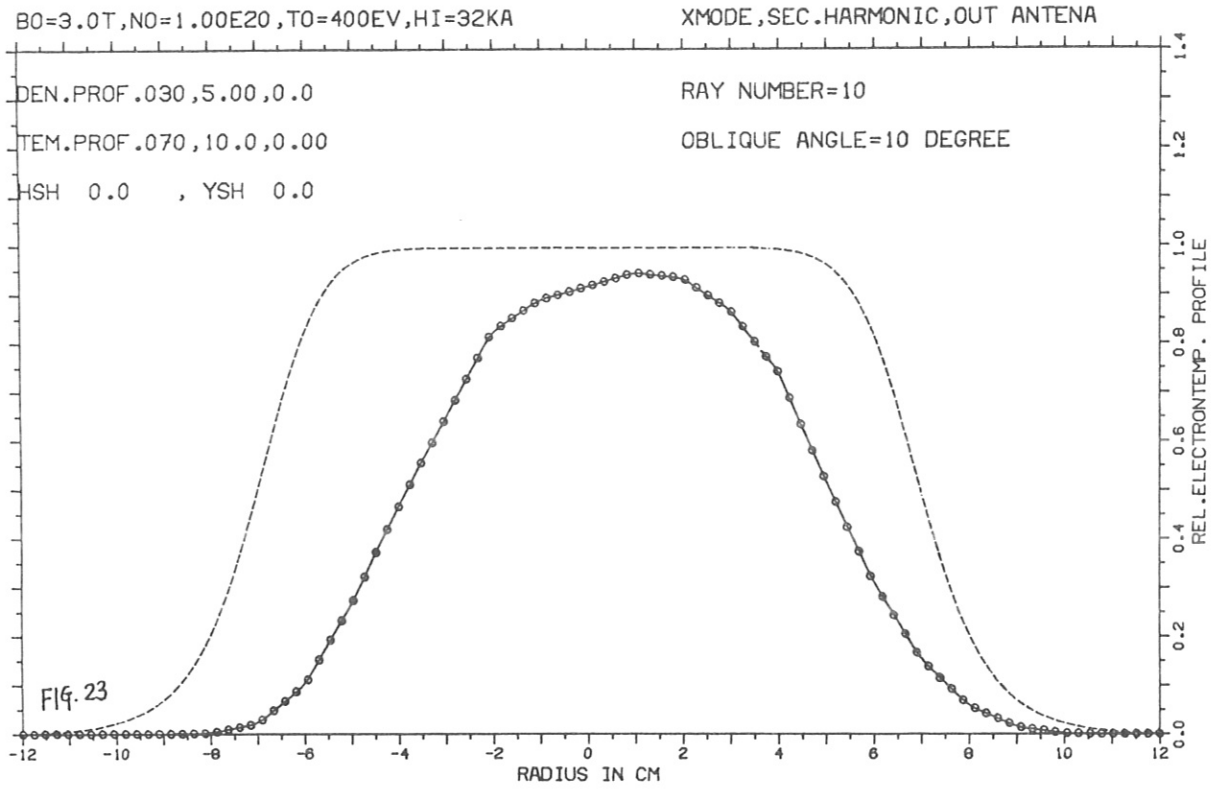


FIG. 23

BO=3.0T,NO=1.00E20,TO=400EV,HI=32KA

XMODE,SEC.HARMONIC,OUT ANTENA

DEN.PROF.030,5.00,0.0

RAY NUMBER=10

TEM.PROF.070,10.0,0.00

OBLIQUE ANGLE=10 DEGREE

HSH 0.0 , YSH 0.0

FREQUENCY=175.2GC

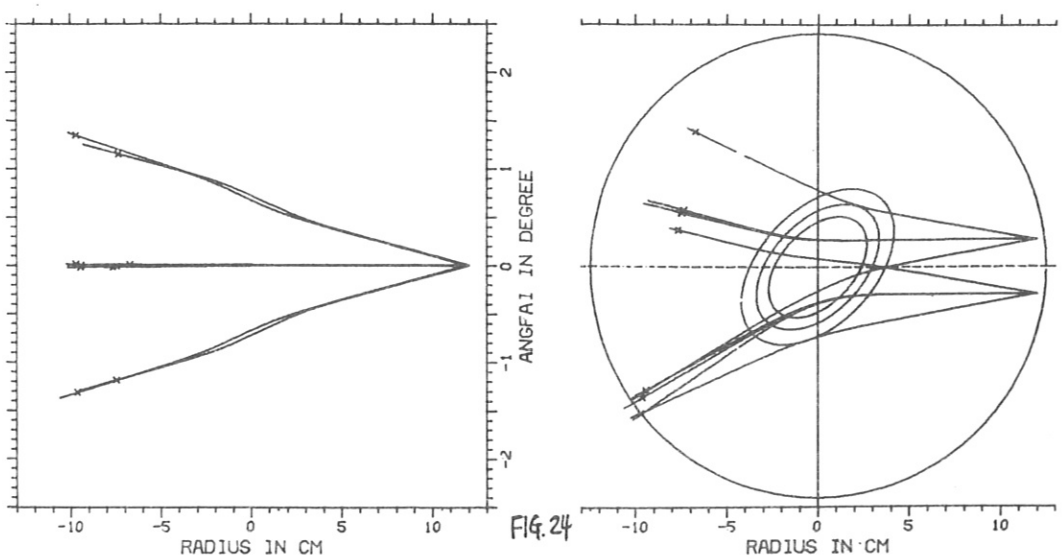


FIG. 24

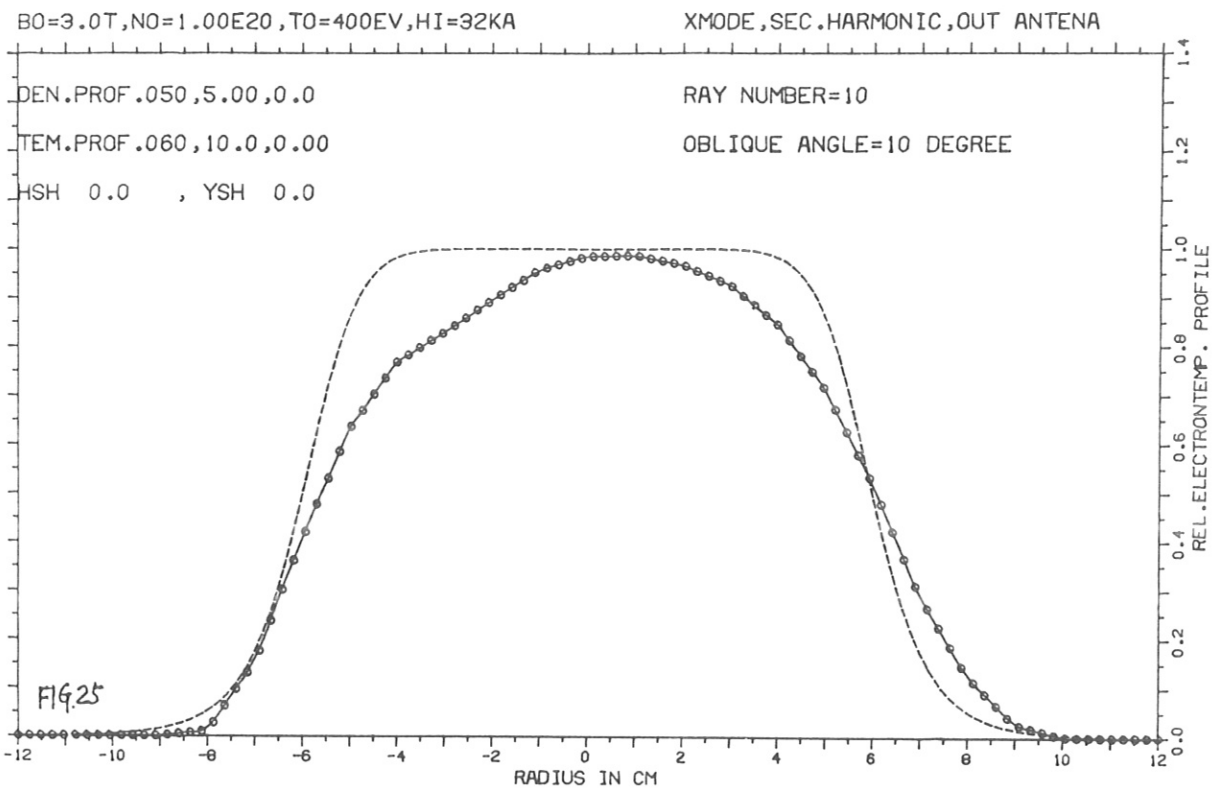
BO=3.0T,NO=1.00E20,TO=400EV,HI=32KA
XMODE,SEC.HARMONIC,OUT ANTENA
DEN.PROF.050,5.00,0.0
TEM.PROF.060,10.0,0.00
HSH 0.0 , YSH 0.0
RAY NUMBER=10
OBLIQUE ANGLE=10 DEGREE
REL.ELECTRONTEMP. PROFILE
RADIUS IN CM
-12 -10 -8 -6 -4 -2 0 2 4 6 8 10 12
0.0 0.2 0.4 0.6 0.8 1.0 1.2 1.4

FIG.25

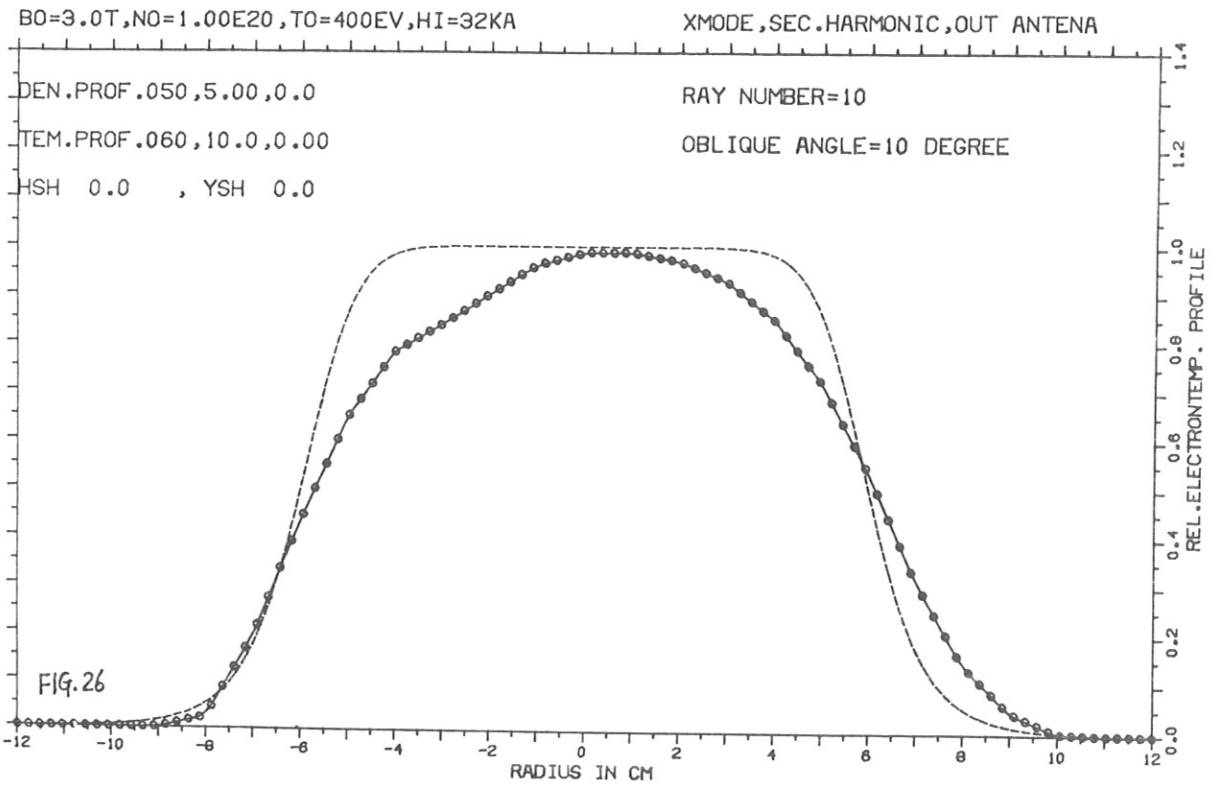
BO=3.0T,NO=1.00E20,TO=400EV,HI=32KA
XMODE,SEC.HARMONIC,OUT ANTENA
DEN.PROF.050,5.00,0.0
TEM.PROF.060,10.0,0.00
HSH 0.0 , YSH 0.0
RAY NUMBER=10
OBLIQUE ANGLE=10 DEGREE
REL.ELECTRONTEMP. PROFILE
RADIUS IN CM
-12 -10 -8 -6 -4 -2 0 2 4 6 8 10 12
0.0 0.2 0.4 0.6 0.8 1.0 1.2 1.4

FIG.26

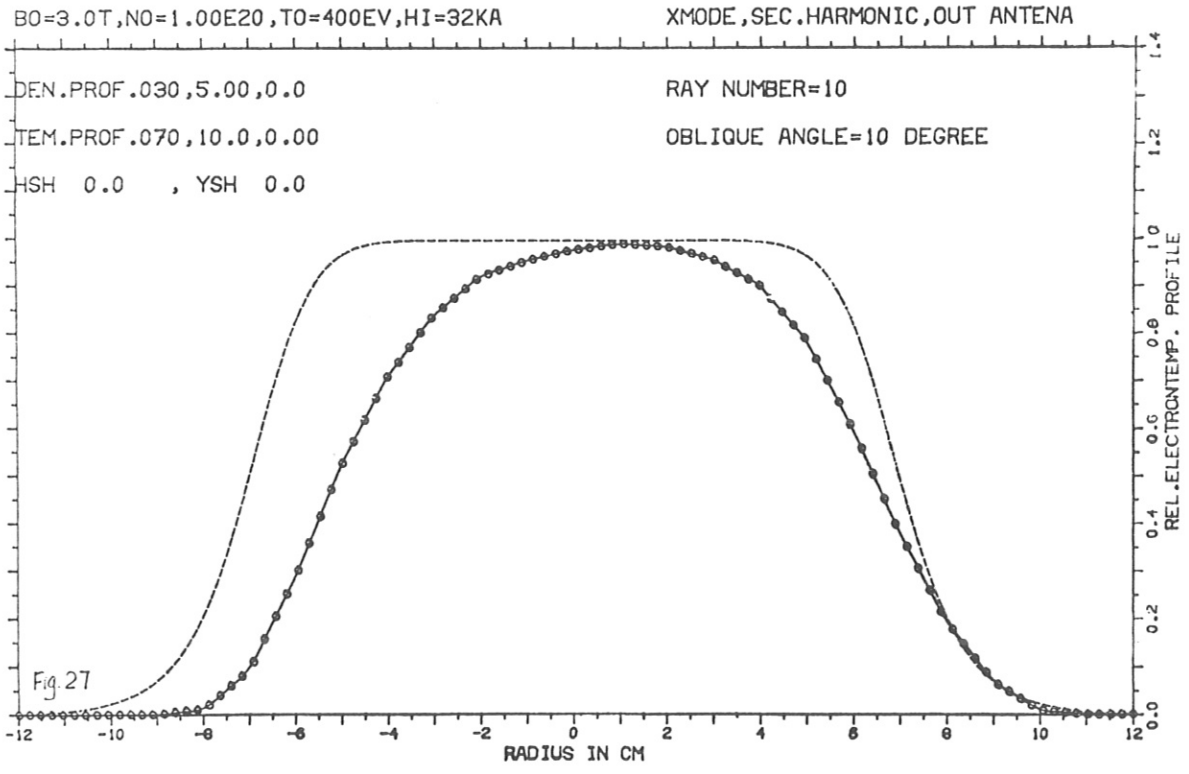
BO=3.0T,NO=1.00E20,TO=400EV,HI=32KA
XMODE,SEC.HARMONIC,OUT ANTENA
DEN.PROF.030,5.00,0.0
RAY NUMBER=10
TEM.PROF.070,10.0,0.00
OBLIQUE ANGLE=10 DEGREE
HSH 0.0 , YSH 0.0
REL.ELECTRONTEMP. PROFILE
RADIUS IN CM
-12
-10
-8
-6
-4
-2
0
2
4
6
8
10
12
0.0
0.2
0.4
0.6
0.8
1.0
1.2
1.4

Fig. 27